Phase Behavior of Near-Monodisperse Semifluorinated Diblock Copolymers by Atom Transfer Radical Polymerization

Tracy L. Bucholz and Yueh-Lin Loo*

Department of Chemical Engineering, Center for Nano- and Molecular Science and Technology (CNM), University of Texas at Austin, 1 University Station, C0400, Austin, Texas 78712

Received May 1, 2006; Revised Manuscript Received June 27, 2006

ABSTRACT: Well-defined diblock copolymers of pentafluorostyrene and methyl methacrylate with narrow molecular weight distributions (PDI < 1.15) were successfully synthesized by atom transfer radical polymerization (ATRP). Both polypentafluorostyrene and poly(methyl methacrylate) can serve as effective macroinitiators for the polymerization of the subsequent block. Because of thermodynamic immiscibility between the two blocks, these diblock copolymers undergo microphase separation upon annealing to form ordered nanostructures. The order−disorder transition temperatures for a series of symmetric, low molecular weight samples were determined to ascertain the temperature dependence of the Flory−Huggins interaction parameter (χ). Poly(pentafluorostyrene-*b*-methyl methacrylate) is only about twice as segregated as its nonfluorinated counterpart, poly(styrene-*b*-methyl methacrylate), or the quintessential poly(styrene-*b*-isoprene), at 440 K. Despite perfluorination of the ring, the symmetric placement of the C−F bonds on the benzene ring causes the polarities at the *ortho* and *meta* positions to cancel in polypentafluorostyrene. Replacing polystyrene with polypentafluorostyrene thus only leads to a small net polarity increase, which in turn results in a reduced polarity difference between polypentafluorostyrene and poly(methyl methacrylate), as compared to that predicted on the basis of the increase in fluorine content alone.

Introduction

Fluoropolymers are interesting because they are chemically inert, are thermally stable, and possess low surface energy, low dielectric constant, and low refractive index.[1] Semifluorinated block copolymers—consisting of both fluorinated and nonflouorinated blocks—are unique hybrid materials because they exhibit common characteristics of fluoropolymers and block copolymers.[2] Recent applications of semifluorinated block copolymers include low surface energy coatings,[3] stimuli-responsive brushes,[4] and surfactants for emulsion polymerizations in supercritical carbon dioxide.[5]

It is well-known that block copolymers with thermodynamically immiscible segments undergo microphase separation to create well-ordered nanostructures of various morphologies depending on their segregation strengths, degrees of polymerization, and relative block lengths.[6] Semifluorinated block copolymers also microphase separate to form nanostructures. Semifluorinated block copolymers, however, are often characterized by large interblock segregation strengths.[7] These materials can therefore potentially exhibit unprecedented phase behavior, particularly in the strongly segregated regime.[8]

The controlled synthesis of semifluorinated block copolymers, however, has been challenging due to the electron-withdrawing nature of the fluorine atoms in the monomers.[9] To overcome this technical barrier, semifluorinated block copolymers are typically made by postpolymerization fluorination of precursors synthesized by anionic polymerization[10,11] or by coupling end-functionalized fluorinated chains to hydrocarbon chains.[6,12] Unfortunately, these polymerization techniques can be tedious and can require a large excess of fluorinated reactants to ensure complete reaction.[6] More recently, reversible addition−fragmentation chain transfer (RAFT) polymerization has been used to make fluorine-containing block copolymers. This technique, however, requires the synthesis of complicated chain transfer agents.[13,14] The advent of atom transfer radical polymerization (ATRP) has allowed the direct synthesis of a variety of semifluorinated block copolymers from commercially available starting materials without any postpolymerization reactions.[15,16] Additionally, ATRP has garnered much attention for its ability to produce well-defined functional polymers under less stringent conditions than traditional living polymerizations.[17−19] ATRP is thus an ideal and facile synthetic approach to creating functional block copolymers with chemically unique segments and narrow molecular weight distributions.

In this work, we report the controlled synthesis of poly(pentafluorostyrene-*b*-methyl methacrylate), PPFS/PMMA, block copolymers using ATRP. The resulting diblock copolymers all have narrow molecular weight distributions (PDI < 1.15), and they undergo microphase separation upon annealing at elevated temperatures to form ordered nanostructures whose details depend on the relative block lengths. The order−disorder transition (ODT) temperatures for a series of low molecular weight, symmetric samples were determined to ascertain the interblock segregation strength, or the Flory−Huggins interaction parameter (χ), as a function of temperature. Our results indicate that PPFS/PMMA is only about twice as segregated as both its nonfluorinated counterpart, poly(styrene-*b*-methyl methacrylate), PS/PMMA, and the quintessential poly(styrene-*b*-isoprene), PS/PI.

Experimental Section

Materials. Methyl methacrylate (MMA, Acros, 99%) and 2,3,4,5,6-pentafluorostyrene (PFS, Acros and Oakwood Chemicals, 97%) were passed through a basic alumina column to remove the inhibitors and stored in the freezer under nitrogen until further use. 1-Bromoethylbenzene (Acros, 97%), ethyl 2-bromoisobutyrate (EBiB, Aldrich, 98%), Cu(I)Br (Aldrich, 98%), $Cu(II)Br_2$ (Aldrich, 98%), *N*,*N*,*N*,*N*-tetramethylethylenediamine (TMEDA, Aldrich, 99.5+%), and *N*,*N*,*N*′,*N*″,*N*″-pentamethyldiethylenetriamine (PMDETA, Aldrich, 99%) were used as received.

Synthesis of Bromine-Terminated Polypentafluorostyrene Macroinitiator by ATRP. PFS (14.1 g, 72.6 mmol), Cu(I)Br (416

* Corresponding author. E-mail: lloo@che.utexas.edu.

10.1021/ma0609679 CCC: $33.50
Published on Web 08/03/2006

mg, 2.90 mmol), Cu(II)Br_2 (32.5 mg, 0.145 mmol), and 30 mL of anisole were added to a 100 mL flask containing a magnetic stir bar. The flask was sealed with a rubber septum, and the solution was degassed with N_2 for 30 min. PMDETA (0.67 mL, 3.05 mmol) was added via a gastight syringe while the mixture was stirring to solvate Cu(I)Br. 1-Bromoethylbenzene (0.40 mL, 2.90 mmol) was then added via a gastight syringe, and the solution was immersed in an oil bath preheated to 110 °C to start the reaction. The reaction was carried out for 90 min, after which the flask was taken out of the oil bath and cooled in an ice bath. The solution was then exposed to air to terminate the polymerization. The polymer solution was then diluted with tetrahydrofuran (THF) and stirred over neutral alumina to remove copper compounds. Upon filtration to remove alumina, the solution was allowed to concentrate before precipitation into methanol. The filtered polymer was dried in vacuo at 30 °C. The number-average molecular weight of this polymer was determined to be 7.8 kg/mol with a polydispersity (PDI) of 1.05 by gel permeation chromatography (GPC) with THF as eluent using a d*n*/d*c* value of 0.040 for PPFS.[20] To synthesize PPFS macroinitiators of different molecular weights, the compositions of the reactants were kept constant, and only the reaction time was altered.

Synthesis of Bromine-Terminated Poly(methyl methacrylate) Macroinitiator by ATRP. MMA (18.8 g, 188 mmol), Cu(I)Br (270 mg, 1.88 mmol), Cu(II)Br_2 (21.0 mg, 0.094 mmol), and 20 mL of toluene were added to a 100 mL flask containing a magnetic stir bar. The flask was sealed with a rubber septum, and the solution was degassed with N_2 for 30 min. TMEDA (0.60 mL, 3.95 mmol) was then added via a gastight syringe while the mixture was stirring to solvate Cu(I)Br. EBiB (0.28 mL, 1.88 mmol) was then added via a gastight syringe, and the solution was immersed in an oil bath preheated to 90 °C to start the reaction. The reaction was carried out for 6 h before the reaction medium was cooled to 0 °C and exposed to air to terminate the polymerization. The PMMA macroinitiator was collected and purified according to the same procedures reported above. The number-average molecular weight of this polymer was determined to be 11.1 kg/mol with a PDI of 1.03 by GPC with THF as eluent using a d*n*/d*c* value of 0.080 for PMMA.[21] To synthesize PMMA macroinitiators of different molecular weights, we altered the reaction times accordingly.

Synthesis of Poly(pentafluorostyrene-*b*-methyl methacrylate) Diblock Copolymers. PPFS macroinitiator (2.5 g, M_n = 7.8 kg/mol), MMA (16.1 g, 160.7 mmol), Cu(I)Br (46.0 mg, 0.32 mmol), Cu(II)Br_2 (3.7 mg, 0.0016 mmol), and 51.3 mL of toluene were added to a 250 mL flask equipped with a magnetic stir bar. The solution was allowed to stir to dissolve the PPFS macroinitiator and then degassed with N_2 for 30 min. TMEDA (0.11 mL, 0.64 mmol) was then added via a gastight syringe while stirring the mixture to solvate Cu(I)Br. The flask was then immersed in an oil bath preheated to 90 °C to start the reaction. The reaction was carried out for 4 h and 15 min before the reaction medium was cooled to 0 °C and exposed to air to terminate the polymerization. The diblock copolymer was collected and purified in the same fashion as reported above. The resulting diblock copolymer has a PDI of 1.09 by GPC with THF as eluent and an absolute molecular weight of 14.2 kg/mol, given the molecular weight of the macroinitiator and compositional analysis by ^{1}H NMR (see Results and Discussion section for greater detail). To synthesize diblock copolymers using PMMA as the macroinitiator, procedures similar to those for making PPFS homopolymers were employed, with the exception that PMMA macroinitiator, instead of 1-bromoethylbenzene, was added at the onset of the polymerization. For simplicity, PPFS/PMMA diblock copolymers will be referred to as A/B *x*/*y* in this paper, where A is the macroinitiator and B is the second block; *x* and *y* are the absolute number-average molecular weights of the macroinitiator and the second block, respectively.

Characterization. ^{1}H NMR spectroscopy was performed in deuterated chloroform on a Varian Unity+ 300 MHz spectrometer. GPC was performed using a Waters 515 HPLC solvent pump, two PLgel Mixed-C columns (5 μm bead size, 300 × 7.5 mm, Polymer Laboratories Inc.), an Optilab DSP interferometric refractometer (Wyatt Technology Corp.), and a DAWN-EOS multiangle laser light scattering (MALLS) detector (λ = 690 nm, Wyatt Technology Corp.) with THF as the eluent (flow rate = 1.0 mL/min, T = 40 °C). Absolute molecular weights of the macroinitiators were determined using d*n*/d*c* values of 0.040 for PPFS[20] and 0.080 for PMMA.[21] Scanning electron microscopy was performed on a LEO 1530 scanning electron microscope using an operating voltage of 1.5 keV. Small-angle X-ray scattering (SAXS) was performed on a Molecular Metrology system with a rotating anode X-ray generator (Bruker Nonius; Cu target, λ = 1.5406 Å) operating at 3.0 kW. The scattered photons were collected on a 2D multiwire Xe-filled detector (Molecular Metrology, Inc.). Zero angle was calibrated using a silver behenate ($CH_3(CH_2)_{20}COOAg$) standard. Temperature ramp experiments were performed using a custom-designed hot stage (Molecular Metrology, Inc.) that was calibrated with high-density polyethylene (HDPE; $T_{m,final}$ = 131 °C) and syndiotactic polystyrene (sPS; $T_{m,final}$ = 271 °C). The final melting temperatures of HDPE and sPS were determined using a Perkin-Elmer DSC 7 at a heating rate of 10 °C/min. To ensure temperature uniformity across the polymer sample during SAXS experiments, aluminum foil in addition to Kapton was used on either side of the polymer specimen as windows. Individual SAXS profiles were collected for 2 h at room temperature and for 30 min at elevated temperatures.

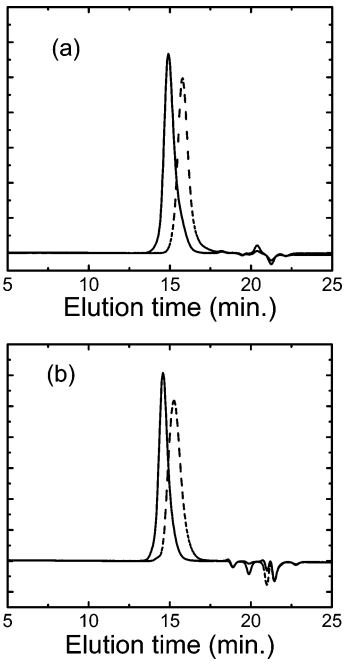

Figure 1. Gel permeation chromatography traces with tetrahydrofuran as the eluent at 1 mL/min: (a) PPFS macroinitiator (7.8 kg/mol, PDI = 1.05; dashed line) and PPFS/PMMA 7.8/14.2 (PDI = 1.09; solid line); (b) PMMA macroinitiator (11.1 kg/mol, PDI = 1.03; dashed line) and PMMA/PPFS 11.1/21.2 (PDI = 1.04; solid line).

Results and Discussion

Figure 1a shows the GPC traces for a PPFS macroinitiator (7.8 kg/mol, dashed line) and PPFS/PMMA 7.8/6.4 (solid line) that was synthesized from the PPFS macroinitiator. We observe a shift to shorter elution times with the diblock copolymer, indicating an increase in molecular weight. In addition, both GPC traces are monomodal and narrow (PDI < 1.15), which are signatures of controlled polymerizations. Figure 1b shows the GPC traces for a PMMA macroinitiator (11.1 kg/mol, dashed line) and PMMA/PPFS 11.1/21.2 (solid line) that was synthesized from the PMMA macroinitiator. In this case as well, the GPC traces confirm the increase in molecular weight and the preservation of the narrow molecular weight distribution when PMMA is used to initiate the polymerization of PFS. For the conditions we have explored, both PMMA and PPFS serve as

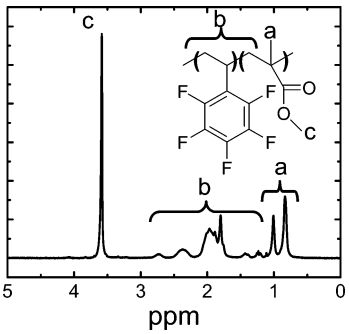

Figure 2. ^{1}H NMR spectrum of PMMA/PPFS 11.1/21.2 in deuterated chloroform. The proton contributions have been labeled for clarity.

effective macroinitiators for the subsequent polymerization of the second block. All the polymerizations were controlled; we did not observe any broadening of the molecular weight distributions by GPC. Figure 2 shows a ^{1}H NMR spectrum of PMMA/PPFS 11.1/21.2 with the appropriate proton contributions labeled. Peaks **a** ($\delta = 0.8$ and 1.0 ppm, 3H) correspond to the protons from the methyl group of PMMA. Peaks **b** ($\delta = 1.2-2.8$ ppm) represent the backbone hydrogens of both PPFS and PMMA. Peak **c** ($\delta = 3.6$ ppm, 3H) arises from the methoxy protons of PMMA. Knowing that three hydrogens from PPFS and two hydrogens from PMMA contribute to peaks **b,** and that three hydrogens from PMMA contribute to peak **c**, the molar fraction of PMMA in the diblock copolymer was determined to be 0.505. We calculated the absolute number-average molecular weight of the diblock copolymer to be $M_n = 32.3$ kg/mol, given the molar composition from ^{1}H NMR and the absolute molecular weight of the macroinitiator from GPC. The volume fraction of PMMA within the diblock copolymer was determined to be 0.407, based on a PMMA density[22] of 1.19 g/cm^3 and a PPFS density of 1.55 ± 0.03 g/cm^3. The density of PPFS was measured using a pycnometer according to ASTM Test D-153-84[23] Method C with water as the nonsolvent. Table 1 lists the pertinent information for all the diblock copolymers used in this study.

Given that these diblock copolymers are narrow in molecular weight distributions, we expect them to form periodic, ordered nanostructures upon microphase separation. Figure 3 shows an SEM micrograph of PMMA/PPFS 11.1/21.2. The SEM specimen was prepared by spin-coating a diblock copolymer solution (10 wt % in ethyl acetate) onto an untreated silicon substrate at 3000 rpm to form a uniform film that is ≅300 nm thick. The film was then annealed at 170 °C for 24 h. Because of the low surface energy of PPFS,[24] the specimen readily forms a PPFS wetting layer at the air−polymer interface during annealing. To remove this surface wetting layer prior to imaging, the surface of the specimen was subjected to reactive ion etching with CF_4.[25] In the micrograph in Figure 3, the PPFS matrix appears bright while the PMMA domains appear dark. The white particles to the right of the micrograph were used to focus the image. This micrograph shows that PMMA/PPFS 11.1/21.2 (40.7 vol % PMMA) forms cylindrical structures under the specimen preparation and annealing conditions. In particular, we observe PMMA cylinders running both in-plane and out-of-plane. For clarity, we have highlighted a small region in the left portion of the micrograph that shows PMMA cylinders oriented out-of-plane. These cylinders appear to be organized on a hexagonal lattice. We note, however, that the microdomains are not very ordered, and the typical grain size observed only spans several hundred nanometers. We speculate that the smaller grain size arises from a combination of the high segregation strength of the diblock copolymer and the relatively low annealing temperature employed.

The morphology ascertained by SEM can be confirmed with bulk structural characterization by SAXS. For SAXS experiments, the diblock copolymers were molded into 0.25 mm thick disks using a melt press at 160 °C. These samples were then annealed overnight at 160 °C, well above the glass transition temperatures of both blocks ($T_{g,PPFS} \approx 105$ °C[26] and $T_{g,PMMA} \approx 100$ °C[27]). Figure 4 provides the one-dimensional SAXS profiles obtained at room temperature of two representative diblock copolymers. The SAXS profile of PMMA/PPFS 11.1/21.2 in Figure 4a shows an intense primary peak at $q^* = 0.332$ nm^{-1} followed by higher-order reflections at q/q^* ratios of $\sqrt{3}$, $\sqrt{4}$, $\sqrt{7}$, and $\sqrt{9}$. Consistent with the micrograph in Figure 3, the relative peak spacings indicate that PMMA/PPFS 11.1/21.2 adopts a hexagonally packed cylindrical morphology. On the basis of the primary peak position and a PMMA volume fraction of 40.7 vol %, we determined a characteristic spacing between the (10) planes of the hexagonal lattice to be 18.9 nm and an average cylinder radius of 7.30 nm. The SAXS profile of PPFS/PMMA 8.5/13.7 in Figure 4b also shows a narrow and intense primary peak at $q^* = 0.354$ nm^{-1}, but with higher-order reflections at q/q^* ratios of 2, 3, and 4, consistent with an alternating lamellar morphology. From the primary peak position, we determined a characteristic lamellar repeat spacing of 17.7 nm. Given that the volume fraction of PMMA is 67.6 vol %, the thickness of the PMMA lamellae is estimated to be 12.0 nm.

On the basis of the classical mean-field diblock copolymer phase diagram predicted by Matsen and Bates,[28] we expected to observe an alternating lamellar morphology for diblock copolymers with volume fractions between 40 and 60%. That PPFS/PMMA 8.5/13.7 exhibits a lamellar morphology despite having 67.6 vol % PMMA suggests that the phase diagram for this diblock copolymer deviates from classical theory. This observation is also consistent for PMMA/PPFS 11.1/21.2. PMMA/PPFS 11.1/21.2 contains of 40.7 vol % PMMA, yet this polymer consistently exhibits a cylindrical structure. In fact, structural characterization on several other PPFS/PMMA diblock copolymers of varying compositions indicate the presence of cylindrical structures at PMMA volume fractions as high as 44% and lamellar structures at PMMA volume fractions as high as 68%. While we are not able to access the ODTs of these diblock copolymers, the morphologies they exhibit appear to be independent of processing history (i.e., solvent-cast vs melt-pressed) and are stable over the entire range of temperatures examined (<300 °C). We speculate that the electron withdrawing nature of fluorine is likely to play a role in skewing the phase diagram. Additionally, conformational asymmetry is also likely to play an important role. This is analogous to that previously reported for PS/PI diblock copolymers.[29]

Order−Disorder Transitions of PPFS−PMMA Lamellar Samples. To examine the segregation strength of PPFS/PMMA, we synthesized a series of symmetric diblock copolymers with accessible ODTs. The physical characteristics of these diblock copolymers are also listed in Table 1. The ODTs for these lamellar samples were determined by SAXS during temperature ramp experiments. After each temperature ramp, the polymer specimens were allowed to equilibrate for 30 min before SAXS acquisition. Figure 5a shows a series of one-dimensional SAXS profiles highlighting the primary peak (q^*) region of PPFS/PMMA 7.8/6.4 at elevated temperatures. The SAXS profiles have been shifted along the y-axis for clarity. We observe that the primary peak broadens and shifts toward lower q with increasing temperature. This phenomenon is quantified in Figure

Table 1. Physical Characteristics of PPFS/PMMA Diblock Copolymers

nomenclature	$M_{n,macro}$[a] (kg/mol)	PDI_{macro}	$M_{n,total}$[b] (kg/mol)	$PDI_{diblock}$	f_{PMMA}[c]	N[d]
PMMA/PPFS 11.1/21.2	11.1	1.03	32.3	1.04	40.7	230.
PPFS/PMMA 8.5/13.7	8.5	1.05	22.2	1.10	67.6	170.
PPFS/PMMA 7.8/6.4	7.8	1.05	14.2	1.12	51.8	98.2
PPFS/PMMA 7.8/6.6	7.8	1.05	14.4	1.09	52.6	99.4
PPFS/PMMA 6.6/5.3	6.6	1.05	11.9	1.09	51.0	87.0

[a] Number-average molecular weight of the macroinitiator; measured by GPC using a dn/dc value of 0.040 for PPFS homopolymer[20] and 0.080 for PMMA homopolymer.[21] [b] Number-average molecular weight of the diblock copolymer; calculated using molar compositions from ^{1}H NMR and known homopolymer M_n from *a*. [c] Volume fraction of PMMA; calculated using molar compositions from ^{1}H NMR and polymer densities of ρ_{PPFS}[23] = 1.55 g/cm^3 and ρ_{PMMA}[22] = 1.19 g/cm^3. [d] Degree of polymerization; calculated using a PS reference volume of 166.3 Å^3.

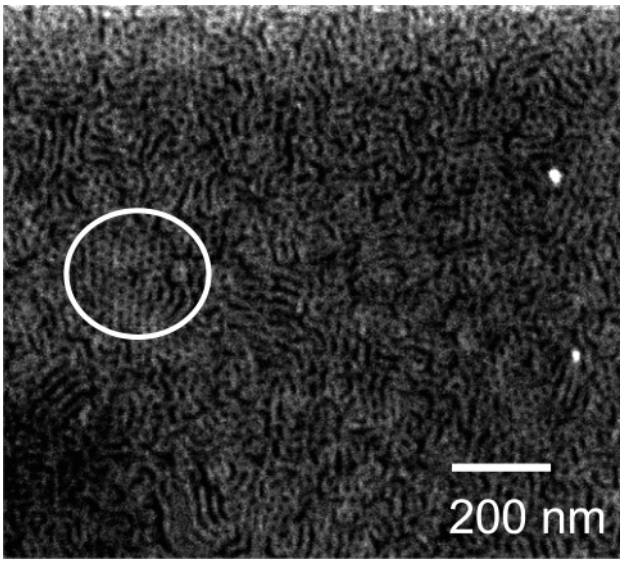

Figure 3. Scanning electron micrograph of PMMA/PPFS 11.1/21.2 indicating a cylindrical morphology. The light regions are PPFS, and the dark regions are PMMA. The highlighted region shows cylinders organized on a hexagonal lattice running in- and out-of-plane.

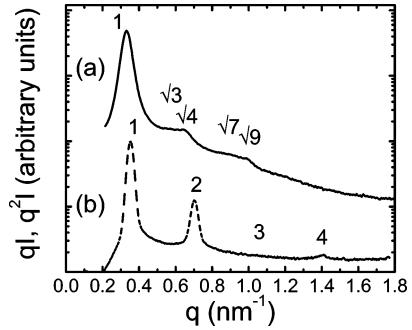

Figure 4. Room temperature small-angle X-ray scattering profiles of (a) PMMA/PPFS 11.1/21.2 and (b) PPFS/PMMA 8.5/13.7. The traces have been shifted along the *y*-axis for clarity. The q/q^* ratios are also labeled.

5b, where q^* and the width of the primary peak at half its maximum intensity are plotted as a function of temperature. We observe that the q^* remains largely constant on heating until 240 °C, where it drops precipitously to $q^* = 0.436$ nm^{-1}. This sharp change in q^* is accompanied by a significant broadening of the primary peak at 240 °C. Both phenomena are indications of disorder, suggesting that this polymer has undergone an ODT at 240 °C. Similar experiments were repeated for two additional lamellar samples. Following the same procedure, we determined that PPFS/PMMA 7.8/6.6 exhibits an ODT at 264 °C and PPFS/PMMA 6.6/5.3 exhibits an ODT at 165 °C. We have also carried out multiple heating and cooling cycles above and below the ODTs, respectively. These temperature changes have always induced disordering and reordering of the lamellar structures accordingly so we are confident that these thermal transitions

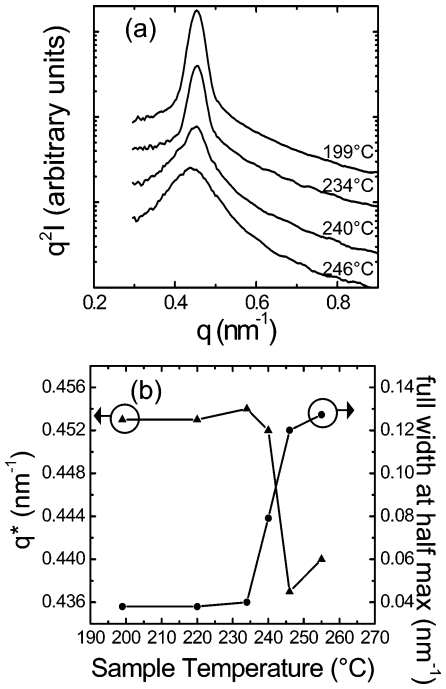

Figure 5. (a) Small-angle X-ray scattering profiles for PPFS/PMMA 7.8/6.4 during a temperature ramp experiment; (b) the primary peak position (q^*, solid triangles) and the primary peak width at half its maximum intensity (solid circles) corresponding to the temperature ramp experiment. The SAXS profiles in (a) have been displaced along the *y*-axis for clarity. This diblock copolymer exhibits an order−disorder transition at 240 °C.

are reversible. Furthermore, ^{1}H NMR and GPC analyses carried out on the diblock copolymers before and after ODT measurements indicate that the samples have not degraded or cross-linked during the experiments.

Interblock Segregation Strength Determination. According to Leibler's mean-field theory,[30] symmetric diblock copolymers disorder when $\chi N = 10.5$, where χ is the Flory−Huggins interaction parameter and measures the segregation strength between the two blocks, and N is the degree of polymerization of the diblock copolymer. Setting $(\chi N)_{ODT} = 10.5$ for our three lamellar samples, we obtained an empirical relationship for χ as a function of temperature in the form $\chi = A/T + B$. For the ease of comparison with χ's previously published for other diblock copolymer systems, we used a polystyrene reference volume of 166.3 Å^3 to calculate N:[31]

$$\chi_{PPFS/PMMA} = \frac{37.3}{T} + 0.0353 \qquad (1)$$

In eq 1, T is in absolute temperature units. The equation above reveals a moderate temperature dependence of the segregation strength (A term) and a relatively small entropic contribution (B term). The temperature dependence of the interblock segregation strength for PPFS/PMMA is plotted in Figure 6.

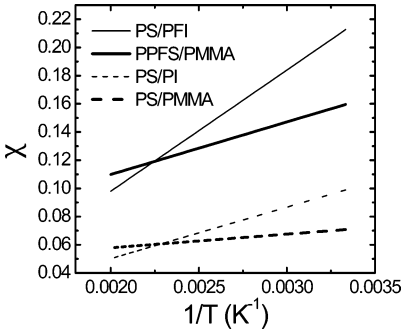

Figure 6. Temperature dependence of the Flory−Huggins interaction parameter for four diblock copolymers extracted using mean-field theory and a polystyrene reference volume of 166.3 Å^3.

For comparison, we have also included the temperature dependence of χ found in the literature for several other common diblock copolymers.[7,31,32] The temperature dependence of χ for all these diblock copolymers were calculated on the basis of mean-field theory,[30] and the calculations assumed a polystyrene reference volume of 166.3 Å^3 for extracting N. In cases where $\chi(T)$ was calculated using different reference volumes,[7,32] we recalculated N and therefore $\chi(T)$ using a polystyrene reference volume of 166.3 Å^3. Comparing the temperature dependence of $\chi_{PPFS/PMMA}$ with that of its nonfluorinated counterpart, $\chi_{PS/PMMA}$, in Figure 6 reveals that replacing PS with PPFS results in a steeper temperature dependence of χ. Perfluorination of the benzene ring, however, only results in a 2-fold increase in the interblock segregation strength over this temperature range (300−500 K).[32]

Previously, Lodge and Hillmyer examined the interblock segregation strength of a series of fluorinated poly(styrene-*b*-isoprene) diblock copolymers where the isoprene units have been fully saturated with difluorocarbene, PS/PFI.[33] These diblock copolymers were made by postpolymerization fluorination of anionically polymerized PS/PI. The chemical structures of the diblock copolymers, along with their interblock segregation strengths at 440 K, are provided in Table 2. We have also plotted the temperature dependence of $\chi_{PS/PFI}$ and $\chi_{PS/PI}$[31] in Figure 6 for comparison. Examining the χ between PS/PFI and PS/PI over the temperature range of interest reveals that fluorination of the isoprene units results in a steeper temperature dependence of χ. More specifically, over the temperature range of interest, $\chi_{PS/PFI}$ is about twice that of $\chi_{PS/PI}$. The authors attribute the increase in the segregation strength to the increase in the polarity difference between the two blocks in PS−PFI as the presence of C−F bonds (two per monomer repeat unit) introduces polarity in the PFI segments.[31,34]

Given Lodge and Hillmeyer's findings, we had originally expected to see a significantly larger segregation strength difference between PFS/PMMA and PS/PMMA because PFS contains more C−F bonds (five) per monomer unit compared to FI. We were therefore surprised to find the interblock segregation strength difference between PFS/PMMA and PS/PMMA to be comparable with that between PS/PFI and PS/PI. Admittedly, χ can also by influenced by the chemical details of the nonfluorinated block (PS vs PMMA in our current comparison). The published solubility parameters of the nonfluorinated species (δ_{PMMA} = 19.98 MPa$^{1/2}$, δ_{PS} = 19.33 MPa$^{1/2}$),[35] however, are similar so differences in the interblock segregation strengths must stem from differences in the polarity of the fluorinated component. Examining the chemical structures of the fluorinated species, PPFS and PFI (provided in Table 2), reveals differences in the placement of the C−F bonds that can potentially contribute to the polarity of the repeat units. In PFI, the two C−F bonds are positioned such that they both contribute to the increase in polarity of the repeat units.[34] In PPFS, however, the polarity at the *ortho* and *meta* positions effectively cancel due to the symmetric placement of the C−F bonds on the six-member ring. As a consequence, only the C−F bond in the *para* position contributes to the overall polarity of PPFS despite having five fluorine substitutions on the ring. It therefore appears that the increase in segregation strength is not only correlated to increases in the fluorine content of one of the blocks. Rather, the increase in segregation strength is more directly correlated with increases in the net polarity difference between the two blocks.

Table 2. Flory−Huggins Interaction Parameter for Five Diblock Copolymers Calculated Using Mean-Field Theory[30]

Nomenclature	Structure	value at 440K[a]
PPFS/PMMA	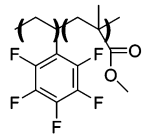	0.120
PS/PMMA	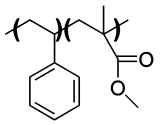	0.061[b]
PS/PFI	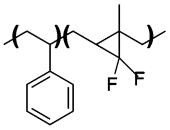	0.121[c]
PS/PI	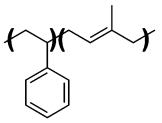	0.060[c]
PB/PFPO	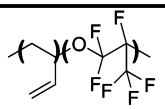	0.353[d]

[a] Using a polystyrene reference volume of 166.3 Å^3. [b] Using data from ref 32. [c] Using data from ref 31. [d] Using data from ref 7.

To substantiate this polarity influence, we also compared the interblock segregation strength of PPFS/PMMA to that of another semifluorinated diblock copolymer with a comparable fluorine content, poly(butadiene-*b*-hexafluoropropylene oxide), PB/PFPO, at 440 K. The chemical structure of PB/PFPO is provided in Table 2; PFPO has six C−F bonds per monomer repeat unit. 440 K was chosen as the point of comparison because the temperature dependence of $\chi_{PB/PFPO}$ was not provided; only $\chi_{PB/PFPO}$ at this temperature was provided in the literature.[7] Prior to comparison, we recalculated $\chi_{PB/PFPO}$ using a polystyrene reference volume of 166.3 Å^3 for consistency. As seen in Table 2, the segregation strength of PB/PFPO is ∼3 times higher than that of PPFS/PMMA despite having comparable fluorine content. The increase in segregation strength compared to PPFS/PMMA can be rationalized by examining the polarity difference between PFPO and PPFS. In PFPO, the C−F bonds are positioned such that the majority of their polarities do not cancel. As such, both the high fluorine content

and the asymmetry of the C−F bonds contribute significantly to the net polarity of PFPO. It is thus not surprising that PB/PFPO has the largest χ among all the diblock copolymers listed in Table 2.

Conclusions

We have successfully synthesized well-defined poly(pentafluorostyrene-*b*-methyl methacrylate) diblock copolymers by atom transfer radical polymerization using either block as a macroinitiator and showed that these diblock copolymers form well-ordered, periodic nanostructures upon annealing. From a series of low molecular weight, symmetric samples, we estimated the temperature dependence of the Flory−Huggins interaction parameter of this system based on mean-field theory. Despite the high fluorine content of PPFS, we demonstrated that PPFS/PMMA is only twice as segregated as both PS/PMMA and PS/PI. This is attributed to the small increase in the net polarity difference between the two blocks.

Acknowledgment. This work is funded by the National Science Foundation (NSF CAREER DMR-0348339) and Camille and Henry Dreyfus New Faculty Award. Support from the Texas Materials Institute is gratefully acknowledged. T.L.B. also thanks the Department of Homeland Security and the Harrington Foundation of the University of Texas at Austin for graduate fellowships.

References and Notes

(1) Li, X.; Andruzzi, L.; Chiellini, E.; Galli, G.; Ober, C. K.; Hexemer, A.; Kramer, E. J.; Fischer, D. A. *Macromolecules* **2002**, *35*, 8078−8087.
(2) Hamley, I. W. *The Physics of Block Copolymers*; Oxford Press: New York, 1998.
(3) Borkar, S.; Jankova, K.; Siesler, H. W.; Hvilsted, S. *Macromolecules* **2004**, *37*, 788−794.
(4) Granville, A. M.; Boyes, S. G.; Akgun, B.; Foster, M. D.; Brittain, W. J. *Macromolecules* **2004**, *37*, 2790−2796.
(5) Canelas, D. A.; Desimone, J. M. *Adv. Polym. Sci.* **1997**, *133*, 103−140.
(6) Bates, F. S. *Science* **1991**, *251*, 898−905.
(7) Zhu, S.; Edmonds, W. F.; Hillmyer, M. A.; Lodge, T. A. *J. Polym. Sci., Polym. Phys. Ed.* **2005**, *43*, 3685−3694.
(8) Davidock, D. A.; Hillmyer, M. A.; Lodge, T. P. *Macromolecules* **2003**, *36*, 4682−4685.
(9) Narita, T. *Macromol. Rapid Commun.* **2000**, *21*, 613−627.
(10) Hillmyer, M. A.; Schmuhl, N. W.; Lodge, T. P. *Macromol. Symp.* **2004**, *215*, 51−56.
(11) Davidock, D. A.; Hillmyer, M. A.; Lodge, T. P. *Macromolecules* **2004**, *37*, 397−407.
(12) Li, Z.; Hillmyer, M. A.; Lodge, T. P. *Macromolecules* **2004**, *37*, 8933−8940.
(13) Ma, Z.; Lacroix-Desmazes, P. *J. Polym. Sci., Polym. Chem. Ed.* **2004**, *42*, 2405−2415.
(14) Pai, T. S. C.; Barner-Kowollik, C.; Davis, T. P.; Stenzel, M. H. *Polymer* **2004**, *45*, 4383−4389.
(15) Radhakrishnan, K.; Switek, K.; Hillmyer, M. A. *J. Polym. Sci., Polym. Chem. Ed.* **2004**, *42*, 853−861.
(16) Zhang, Z. B.; Ying, S. K.; Hu, Q. H.; Xu, X. D. *J. Appl. Polym. Sci.* **2002**, *83*, 2625−2633.
(17) Matyjaszewski, K.; Xia, J. *Chem. Rev.* **2001**, *101*, 2921−2990.
(18) Guice, K.; Loo, Y.-L. *Macromolecules* **2006**, *39*, 2474−2480.
(19) Smith, Q.; Huang, J.; Matyjaszewski, K.; Loo, Y.-L. *Macromolecules* **2005**, *38*, 5581−5586.
(20) Average d*n*/d*c*; obtained from solutions of known PPFS concentrations and assuming 100% mass recovery.
(21) Brandrup, J., Immergut, E. H., Grulke, E. A., Eds.; *Polymer Handbook*, 4th ed.; Wiley-Interscience: New York, 1999; p VII-571.
(22) Brandrup, J., Immergut, E. H., Grulke, E. A., Eds.; *Polymer Handbook*, 4th ed.; Wiley-Interscience: New York, 1999; p VI-13.
(23) ASTM D153-84, Standard Test Methods for Specific Gravity of Pigments, 2003.
(24) Jankova, K.; Hvilsted, S. *J. Fluorine Chem.* **2005**, *126*, 241−250.
(25) Popova, K.; Spassova, E.; Zhivkov, I.; Danev, G. *Thin Solid Films* **1996**, *274*, 31−34.
(26) Granville, A. M.; Boyes, S. G.; Akgun, B.; Foster, M. D.; Brittain, W. J. *Macromolecules* **2005**, *38*, 3263−3270.
(27) Brandrup, J., Immergut, E. H., Grulke, E. A., Eds.; *Polymer Handbook*, 4th ed.; Wiley-Interscience: New York, 1999; p VI-203.
(28) Matsen, M. W.; Bates, F. S. *Macromolecules* **1996**, *29*, 1091−1098.
(29) Lai, C.; Russel, W. B.; Register, R. A.; Marchand, G. R.; Adamson, D. H. *Macromolecules* **2000**, *33*, 3461−3466.
(30) Leibler, L. *Macromolecules* **1980**, *13*, 1602−17.
(31) Ren, Y.; Lodge, T. P.; Hillmyer, M. A. *Macromolecules* **2000**, *33*, 866−876.
(32) Stühn, B. *J. Polym. Sci., Polym. Phys.* **1992**, *30*, 1013−1019.
(33) Ren, Y.; Lodge, T. P.; Hillmyer, M. A. *Macromolecules* **2002**, *35*, 3889−3894.
(34) Hillmyer, M. A.; Lodge, T. P. *J. Polym. Sci., Polym. Chem. Ed.* **2002**, *40*, 1−8.
(35) Utracki, L. A.; Simha, R. *Polym. Int.* **2004**, *53*, 279−286.

MA0609679